C. R. Mecanique 340 (2012) 565–574

Contents lists available at SciVerse ScienceDirect

Comptes Rendus Mecanique

www.sciencedirect.com

Emerging crack front identification from tangential surface displacements

Stéphane Andrieux [a,*], Thouraya Nouri Baranger [b]

[a] LaMSID, UMR CNRS-EDF 2832, 1, avenue du Général de Gaulle, 92141 Clamart cedex, France
[b] Université de Lyon, CNRS, Université Lyon 1, LaMCoS UMR5259, 69621 Villeurbanne cedex, France

ARTICLE INFO

Article history:
Received 9 May 2012
Accepted after revision 11 June 2012
Available online 4 July 2012

Keywords:
Solids and structures
Inverse problem
Crack identification
Cauchy problem
Elasticity
Full-fields measurements
Data completion

Mots-clés :
Solides et structures
Problèmes inverses
Identification de fissure
Problème de Cauchy
Elasticité
Mesures de champs
Complétion de données

ABSTRACT

We present in this Note an identification method for the crack front of a crack emerging at the surface of an elastic solid, provided displacements field or its tangential components are given on a part free of loading of the external surface. The method is based on two steps. The first one is the solution of a Cauchy problem in order to expand the displacement field within the solid up to a surface enclosing the unknown crack. Then the reciprocity gap method is used in order to determine the displacement jump on the crack and then the crack itself. We prove then an identifiability result. The method is illustrated with two synthetic examples: a crossing crack with linear crack front and an elliptic emerging crack.

RÉSUMÉ

On présente dans cette Note une méthode d'identification du front d'une fissure débouchant à la surface d'un solide élastique, à partir de la donnée des composantes tangentielles du champ de déplacement sur une partie libre de charge de la surface extérieure. La méthode comporte deux étapes. Dans un premier temps, on résoud un problème de Cauchy pour prolonger le champ en surface jusqu'à une surface englobant la fissure inconnue. Dans une seconde étape, on utilise la méthode d'écart la réciprocité pour identifier le saut de déplacement à la traversée de la fissure, ce qui conduit, par l'identification du support, à l'identification de la fissure elle-même. On prouve ainsi un résultat d'identifiabilité. La méthode est illustrée sur deux exemples synthétiques : une fissure traversante à front rectiligne et une fissure elliptique débouchante.

1. Introduction

The development of image correlation techniques for digital image cameras (DIC) makes it possible to obtain the displacement field on parts of the surface of a deformed solid [1,2]. The precision and the amount of available data have led to revisit various identification or inverse problems originally based on the fitting of sparse and discrete data. Considering that full field data are available on the boundary, it is possible to replace these problems in the continuum framework in order to derive new solution methods, such as reciprocity methods and Cauchy or data completion problems, methods that will be used in this Note.

Applications of the Cauchy problem in three-dimensional linear fracture mechanics have been recently developed [3] when the geometry of the crack is known. In this article, a constructing method is designed for determining the crack

* Corresponding author.
E-mail addresses: Stephane.Andrieux@edf.fr (S. Andrieux), Thouraya.baranger@univ-lyon1.fr (T.N. Baranger).

1631-0721/$ – see front matter
http://dx.doi.org/10.1016/j.crme.2012.06.002

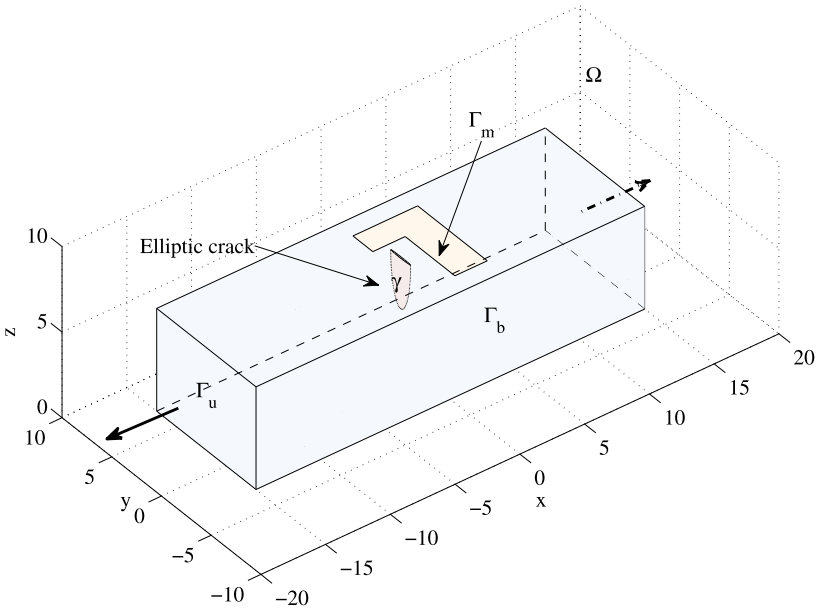

Fig. 1. The generic problem.

geometry, that is the crack front, for plate-like linearly elastic solids and tangential displacement measurements on one side of it. We prove in passing an identifiability result. The applications aimed at here are non-destructive evaluation procedures for the identification of the depth of emerging cracks and monitoring of crack propagation in fatigue tests.

2. Statement of the problem

Consider the solid in Fig. 1 which occupies a three-dimensional domain Ω with height $2H$ and a regular boundary $\partial\Omega$ with outwards unit normal $\mathbf{n}$. It contains a planar crack $\gamma = \gamma^+ \cup \gamma^-$, where γ^+ and γ^- are the two faces of the crack, and $\mathbf{N}$ the outwards unit normal to the face γ^-. Hereafter, we consider only emerging cracks. Therefore the plane where the crack is located is assumed to be known beforehand.

The solid is homogeneous, isotropic and linearly elastic, the fourth order Hooke tensor is denoted by $\mathcal{A}$. The solid is submitted to a loading on some part of its external surface, the crack lips being free of any mechanical loading. The external surface tractions $\sigma.\mathbf{n}$ are not entirely known, then we denote by Γ_b the part of $\partial\Omega$ where this boundary condition is given and we denote by Γ_u the part where all boundary conditions are missing. On another part Γ_m of $\partial\Omega$, which is free of loading $\sigma.\mathbf{n} = 0$, some DIC measurements can be performed, so that the displacement field U^m or only its tangential part denoted by U_t^m is known. The crack does not intersect this measurement surface. The problem can be stated as follows:

Given the overspecified boundary data $(U_t^m, \sigma.\mathbf{n} = 0)$ *on* Γ_m*, to identify the emerging planar crack, that is the plane domain* γ*.*

Let us comment briefly the fact that the measurement surface does not meet the crack intersection with the external surface of the solid. Because of displacement discontinuities are likely to occur across the crack surface, usual image correlation techniques which rely on regularity assumptions on the displacement field are not suited to deal with this kind of situation. It must be restricted to parts where the regularity assumptions are valid. Some authors [4,5] developed special methods in order to include the possibility of discontinuous displacements across a line but it usually requires the knowledge of the direction of the line and of the position of the crack tip, sometimes very difficult to achieve, or necessitate non-linear sophisticated algorithms.

Using the data completion problem as a mean for the identification of planar cracks has yet been used by [6], but for a very special situation when the solid is decomposed into to parts being on each side of the crack plane and when data are available in such a way that two data completion problems can be formulated for each of these subdomains.

3. A two steps identification procedure

3.1. Principle

To solve the above problem, a two steps procedure will be used. First, the displacement field given on the part Γ_m of the external surface is expanded within a subdomain Ω_1 of the original domain Ω, excluding a cylindrical domain Ω_2 containing the crack γ, such that $\Omega = \Omega_1 \cup \Omega_2$. This extension or continuation is performed via the solution of a data

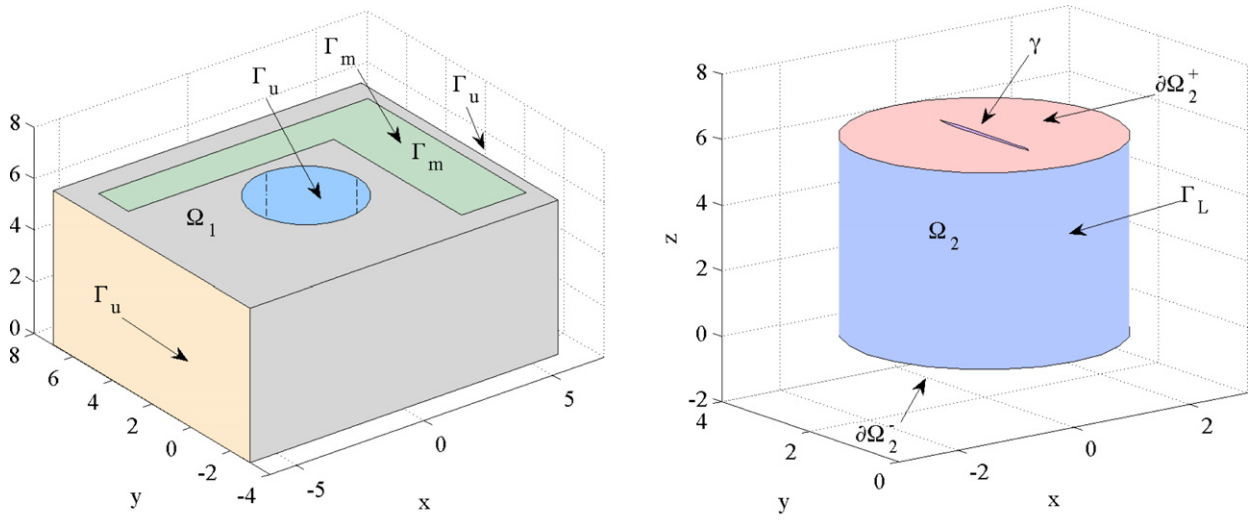

(a) The Domain where Data Completion is achieved (b) The domain where the crack is identified

Fig. 2. Geometries and boundary definitions for the two steps.

completion problem [7–9] which is a form of the Cauchy problem and leads to the determination of the whole displacement field and the stress vector field on a surface Γ_u enclosing the crack. Secondly, equipped with these fields, the crack domain is identified by using the reciprocity gap method [10], which is adapted in order to deal with the lack of knowledge of the displacement field on the upper and lower free surfaces of the boundary of the cylindrical domain Ω_2. Fig. 2 shows the subdomains Ω_1 and Ω_2 and their related boundaries. Notice that normally, the cylindrical part of the boundary Γ_u, which represents the hole's surface in the domain Ω_1, is the same as that of the subdomain Ω_2: $\Omega_1 \cap \Omega_2 = \Gamma_L$. However, for the reciprocity gap computation the subdomain enclosing the crack could be chosen larger than Ω_2 as shown in Fig. 7.

3.2. Solution of the data completion problem

The displacement field u throughout the solid satisfies the equilibrium condition, the constitutive elastic relation, and the associated stress tensor field meets the boundary condition on $\Gamma_b \cap \partial\Omega_1$. Furthermore, boundary conditions have to be fulfilled on the part Γ_m where the measurements are performed. The set of equations is then:

$$\begin{cases} div\,\sigma(u) = 0 & \text{in } \Omega_1 \\ \sigma(u) = \mathcal{A} : \varepsilon(u) & \text{in } \Omega_1 \\ \sigma(u).\mathbf{n} = b & \text{on } \Gamma_b \cap \partial\Omega_1 \\ \sigma(u).\mathbf{n} = 0, \quad u - u.\mathbf{n} = U_t^m & \text{on } \Gamma_m \end{cases} \tag{1}$$

Expanding the data within the solid Ω_1 is reformulated as the following data completion problem:

Find (U, T) *on the remaining part* Γ_u *of the boundary of the domain* Ω_1, *such that a displacement field u exists, satisfying* (1) *and the conditions on* Γ_u:

$$\sigma(u).\mathbf{n} = T, \qquad u = U \tag{2}$$

Strictly speaking, the problem of determining a displacement field satisfying the equations set (1) is a Cauchy problem. More precisely the problem tackled with here has been called an incomplete Cauchy problem because only the tangential part of the displacement field is given on Γ_m. The determination the pair (U, T) is a data completion problem. Both problems are ill posed. Firstly because the given data on Γ_m must be compatible, a condition that is not explicit, meaning that all pairs of $H^{1/2}(\Gamma_m)^3 \times H^{-1/2}(\Gamma_m)^3$ do not lead to a solution of the Cauchy or data completion problem. It can nevertheless be proven [11] that the subset of compatible pairs is dense in $H^{1/2}(\Gamma_m)^3 \times H^{-1/2}(\Gamma_m)^3$. Secondly, the two problems are ill posed because of the lack of continuity of the solution, when it exists, with respect to the data pair $(U_t^m, \sigma.\mathbf{n} = 0)$.

To solve the data completion problem, we use a special version of the energy error gap method [8]. It has two steps. First two elastostatic problems are defined on the domain Ω_1 with solutions u_1 and u_2:

$$\begin{cases} div\,\sigma(u_1)=0 & \text{in } \Omega_1 \\ \sigma(u_1)=\mathcal{A}:\varepsilon(u_1) & \text{in } \Omega_1 \\ \sigma(u_1).\mathbf{n}=b & \text{on } \Gamma_b \\ u_1-(u_1.\mathbf{n})\mathbf{n}=U_t^m & \text{on } \Gamma_m \\ \sigma(u_1).\mathbf{n}=\eta & \text{on } \Gamma_u \end{cases} \quad \begin{cases} div\,\sigma(u_2)=0 & \text{in } \Omega_1 \\ \sigma(u_2)=\mathcal{A}:\varepsilon(u_2) & \text{in } \Omega_1 \\ \sigma(u_2).\mathbf{n}=b & \text{on } \Gamma_b \\ \sigma(u_2).\mathbf{n}=0 & \text{on } \Gamma_m \\ \sigma(u_2).\mathbf{n}=\eta & \text{on } \Gamma_u \end{cases} \tag{3}$$

The normal traction vector η in $H^{-1/2}(\Gamma_u)^3$ is taken as the unknown of the problem. If $u_1(\eta)=u_2(\eta)+R_B$ then the data completion problem has the solution:

$$T=\eta, \qquad U=u_1|_{\Gamma_u}+R_B|_{\Gamma_u} \tag{4}$$

where R_B is a rigid body motion belonging to the (possibly empty) subspace of such displacements satisfying the condition of zero tangential displacement on the measurement surface Γ_m:

$$\left\{R_B=\mathbf{t}+\mathbf{r}\wedge\mathbf{x},\ (\mathbf{t},\mathbf{r})\in\mathcal{R}^6,\ R_B-(R_B.\mathbf{n})\mathbf{n}=0 \text{ on } \Gamma_m\right\} \tag{5}$$

Then, as a second step, the normal traction vector field η is determined by minimising an error gap between $u_1(\eta)$ and $u_2(\eta)$. This gap is chosen as an energy gap. The data completion problem is then solved via the following optimisation problem:

$$T=\underset{\eta\in H^{-1/2}(\Gamma_u)^3}{\arg\min}\,E(\eta) \tag{6}$$

$$\text{with } E(\eta)=\int_{\Omega_1}\mathcal{A}:\varepsilon(u_1-u_2):\varepsilon(u_1-u_2)\,d\Omega_1, \quad q\big(u_1(\eta),u_2(\eta)\big) \text{ given by (3)} \tag{7}$$

One can easily show [7] that for a compatible data pair $(U_t^m,\sigma(u).\mathbf{n}=0)$, the functional E is positive, quadratic, convex and zero if $u_1(\eta)$ and $u_2(\eta)$ differ only by a rigid body motion of R_B, which leads to the results (4). The solution of the Cauchy problem is $u_1(T)$. The minimisation of E has nevertheless to be conducted with care as the data completion problem is ill posed. In particular the discrete gradients have to be computed with adjoint methods and trust-region algorithms are to be used, see [11] for details. Let us note that no regularisation is incorporated although it could be considered as unavoidable in the solution procedure for ill-posed problems. Numerical experiments have shown that within a noise range less than 5% on the data, the regularisation brought by an ad hoc stopping criterion is sufficient as shown in [12]. Notice that the situation is favourable here because of the nullity of one of the data. This noise level is currently obtained with DIC image correlation techniques.

4. Identification of the crack front by the reciprocity gap method

Once the displacement field U_L and the traction vector field T_L are determined on the Γ_L surface, the reciprocity gap method can be applied in order to identify the crack domain γ and the crack front. The reciprocity gap functional is here defined as the following linear form acting on $H^1(\Omega_2)^3$, that is on regular fields v defined on the uncracked domain:

$$RG(v)=\int_{\Gamma_L}\left[T_L.v-\sigma(v).\mathbf{n}.U_L\right]dS \tag{8}$$

This definition uses only known quantities on the lateral side of the domain Ω_2 and the computation of RG on any v field involves only a boundary integral. Using the elastic equilibrium equation in $\Omega_2\setminus\gamma$ for the real displacement field $\mathbf{u}$, it is straightforward to show the following property of the reciprocity gap functional on the subspace of elastic equilibrium fields in Ω_2, with vanishing traction vector on the upper and lower sides Ω_2^+ and Ω_2^- of Ω_2, as depicted in Fig. 2b:

$$RG(v)=\int_{\gamma}\sigma(v).\mathbf{n}.[\![u]\!]\,dS, \quad \forall v:\ div\,\sigma(v)=0 \text{ in } \Omega_2 \text{ and } \sigma(v).\mathbf{n}=0 \text{ on } \Omega_2^+\cup\Omega_2^- \tag{9}$$

$[\![u]\!]$ denotes the actual displacement jump across the crack.

As mentioned before, we consider only emerging cracks. Therefore the plane where the crack is located is assumed to be known beforehand. Let us now define $\rho=[0,2R]\times[0,2H]$, the rectangle resulting from the intersection of the crack plane Π and the domain Ω_2 as shown in Fig. 3, and then specialise the v fields in the following $\mathbb{N}^2$ parametrised family:

$$v^{mn}(x,y,z)=\begin{bmatrix} \frac{m\pi}{2R\lambda_{mn}}\sin(\frac{m\pi y}{2R})\cos(\frac{n\pi z}{2H})\sinh(\lambda_{mn}x) \\ \cos(\frac{m\pi y}{2R})\cos(\frac{n\pi z}{2H})\cosh(\lambda_{mn}x) \\ 0 \end{bmatrix} \quad \text{with } \lambda_{mn}=\frac{\pi}{2}\sqrt{\frac{m^2}{R^2}+\frac{n^2}{H^2}} \tag{10}$$

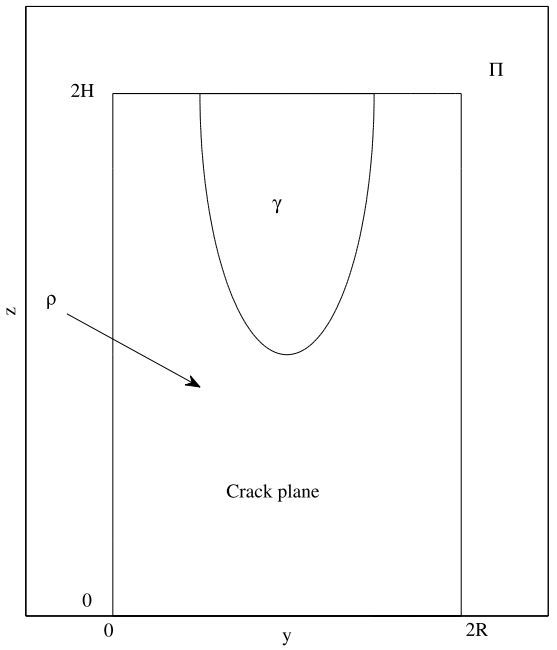

Fig. 3. The definition of the rectangular domain ρ in the Π plane, containing the crack surface.

It is easily seen that the v^{mn} fields are divergence-free (then $Tr(\varepsilon(v^{mn}))$ vanishes), and that each component is harmonic. It is then deduced first that the fields v^{mn} satisfy the Navier equation because this equation involves only the Laplacian of the displacement components and the gradient of its divergence. Secondly, the associated stress tensor by the Hooke's law takes the simple form: $\sigma(v^{mn}) = 2\mu\varepsilon(v^{mn})$ where μ is the Lamé shear modulus.

Because the traction vector also vanishes identically when $z = 0$ and $z = 2H$, that is on the upper and lower faces of the domain Ω_2, the v^{mn} fields can be used in Eq. (9). This leads to the following expressions, where the continuation by zero throughout the rectangular domain ρ of the function $[\![u_x]\!]$ is denoted by $[\![\tilde{u}_x]\!]$:

$$\int_{\rho} [\![\tilde{u}_x]\!](y,z) \sin\left(\frac{m\pi y}{2R}\right) \cos\left(\frac{n\pi z}{2H}\right) \mathrm{d}y\,\mathrm{d}z = \frac{R}{\mu m\pi} RG\left(v^{mn}\right) \tag{11}$$

This equation shows that the components u^{mn} in the series expansion of the function $[\![\tilde{u}_x]\!]$:

$$[\![\tilde{u}_x]\!](y,z) = \sum_{m,n} u^{mn} \sin\left(\frac{m\pi y}{2R}\right) \cos\left(\frac{n\pi z}{2H}\right) \tag{12}$$

can be determined by computing the reciprocity gap on fields of the v^{mn} family. Considering now the following spectral problem for the Laplacian operator on the rectangular domain ρ:

$$\begin{cases} -\Delta\phi = \lambda\phi & \forall (y,z) \in]0,2R[\times]0,2H[\\ \phi = 0 & \forall y \in]0,2H[,\ y = 0, 2R \\ \dfrac{\partial\phi}{\partial n} = 0 & \forall z \in]0,2R[,\ z = 0, 2H \end{cases} \tag{13}$$

it is straightforward to verify that the eigenfunctions ϕ are precisely the functions $(\sin(\frac{m\pi y}{2R})\cos(\frac{n\pi z}{2H}))_{m,n}$ establishing that this function set forms a Hilbertian basis of $L^2(\rho)$ [13] and justifying then the series expansion (12). The formula (11) allows us to claim that the function $[\![\tilde{u}_x]\!]$ can be entirely determined by the data on the lateral surface only of the domain enclosing the crack. The support of this function can be shown to be exactly the γ domain [10] so that (11) proves:

Identifiability property. *The crack domain is identifiable by only one set of lateral overspecified elastic data provided that the normal discontinuity of displacement on the crack does not identically vanish.*

We prove then also that the crack domain is identifiable provided the tangential displacement field on a part of the external surface of the solid is given.

In order to extract the support of the approximation of the function $[\![\tilde{u}_x]\!]$, obtained in practice by a truncated series expansion up to (M, N) and denoted by $[\![\tilde{u}_x]\!]_{MN}$, the indicator function I_γ of the crack domain is finally deduced by the following truncation formula where H is the Heaviside function and δ a small positive scalar:

$$I_\gamma(y,z) \cong H\left(\left|[\![\tilde{u}_x]\!]_{MN}(y,z)\right| - \delta\right) \tag{14}$$

A practical way of choosing the scalar δ is to look for the minimum value that leads to a simply connected domain for the approximation of γ.

5. Numerical examples

In order to illustrate the efficiency of the presented method, we consider a solid as that described in Fig. 1: $30 \times 10 \times 6$ mm. Two cases were studied. In the first case, the solid has at its middle a traversing rectangular crack. In the second case, an elliptic emerging crack is considered. The material is steel with Young modulus $E = 2.1$ GPa and Poisson ratio $\nu = 0.3$. To perform these two numerical experiments, synthetic Cauchy data were generated by solving well-posed forward problems, using finite element modelling with Comsol [14] and Matlab [15] softwares. The mesh sizes and their distributions used for the forward problems are different from that which were used to perform Data Completion and RG approach.

5.1. Traversing rectangular crack

In this example a rectangular 3×6 mm crack is considered. The crack is emerging at the top, the bottom and at the xz-face (for $y = 7$ mm) of the solid. It is located at the middle of the solid following the x-axis. The data completion was carried out on the holed solid with a hole diameter of 3 mm. The forward problem was modelled by 4384 hexahedral and prism finite elements with quadratic Lagrangian interpolation: 10 230 degrees of freedom. Whereas the data completion problem was modelled by 2208 hexahedral and prism finite elements with quadratic Lagrangian interpolation: 6150 degrees of freedom.

The boundary conditions are: the first yz-face Γ_{bl} is clamped whereas on the second yz-face Γ_{br} a displacement following the x-axis is prescribed: $u_x = 0.01$, $u_y = 0$ and $u_z = 0$. The Cauchy data, free traction and displacements, are prescribed on the patches denoted by Γ_m, as shown in Fig. 7. The cylindrical boundary of the hole is Γ_u where the Neumann boundary condition η has to be identified.

When the data completion was achieved, the computation of the displacement jump $[\![\tilde{u}_x]\!]$ is performed by considering a cylindrical domain containing the crack front and which is larger than the hole of Ω_1, such that the boundary Γ_L is inside the subdomain Ω_1 and $\Gamma_u \neq \Gamma_L$, as show in Figs. 2b and 7. This avoids to use directly the identified data on Γ_u, and the integral computation in (8) is performed on the boundary Γ_L.

Figs. 4, 5 and 6 show the computed displacement jump $[\![\tilde{u}_x]\!]$. The first, Fig. 4a, shows the displacement jump computed with the reference model whereas the second, Fig. 5a, shows that computed after data completion process using the Cauchy data on Γ_m. The displacement jump represented in Fig. 6a was obtained after data completion process by considering Dirichlet Cauchy data on Γ_m are noisy (5%). Remark that the Dirichlet Cauchy data was already noisy before adding 5% of white noise, this is due to the numerical noise resulting from the data completion process. Figs. 4b, 5b and 6b show the cross-section of displacement jump in the yx-plane. The crack front is identified by means of the truncation formula $I_\gamma = H(|[\![\tilde{u}]\!]| - \delta)$. The scalar δ is chosen such that the identified domain γ is a simply connected area. For this example we follow the following procedure: for each $M \times N$ value the displacement gap (12) is analysed, then the oscillations are truncated so that (12) represents a simply connected area, this is shown in Figs. 4b, 5b and 6b by the dashed lines. The procedure is stopped when the oscillations of height frequencies become too important and do not allow us to identify a simply connected area.

The reader can observe that, even with noisy Cauchy data, the identified crack front is in good agreement with the reference one.

5.2. Emerging elliptic crack

In this trial, an elliptic front crack is considered as shown in Figs. 1 and 3. Fig. 7 shows the domain used to perform the data completion. The boundary Γ_{bl} is clamped while on Γ_{br} the following displacements are imposed: $u_x = 0.01$, $u_y = 0$ and $u_z = 0$. The crack is 2 mm long and 3 mm deep. Notice that the inner cylindrical boundary Γ_u is that where the Neumann boundary condition is identified, while the boundary Γ_L is that where the *RG* defined by (8) is computed following. The forward problem was modelled by 6317 tetrahedral finite elements with quadratic Lagrangian interpolation: 30 891 degrees of freedom. Whereas the data completion problem was modelled by 5120 tetrahedral finite elements with quadratic Lagrangian interpolation: 26 304 degrees of freedom.

Figs. 8, 9 and 10 show the displacement jump $[\![\tilde{u}_x]\!]$ obtained, respectively, with the reference model and after the data completion process without noise and then with 2% of noise rate. The elliptic crack front is identified by means of the truncation formula $I_\gamma = H(|[\![\tilde{u}]\!]| - \delta)$. The scalar δ is chosen again such that the identified domain γ is a simply connected

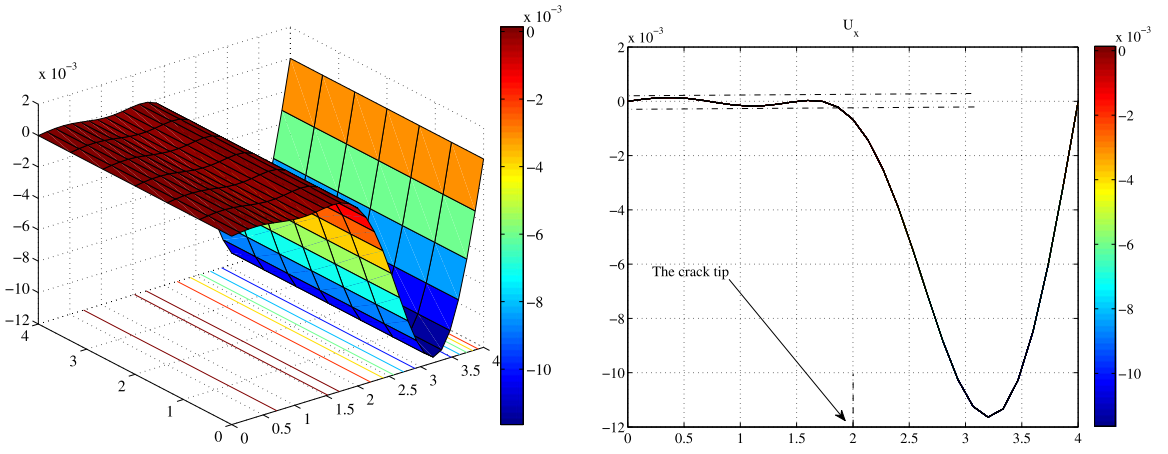

(a) Three dimensional view (b) Cross sectional view in the yx-plane.

Fig. 4. Displacement jump $[\![\tilde{u}_x]\!]$ across the crack of the reference solution. The dashed lines show how the truncation was done.

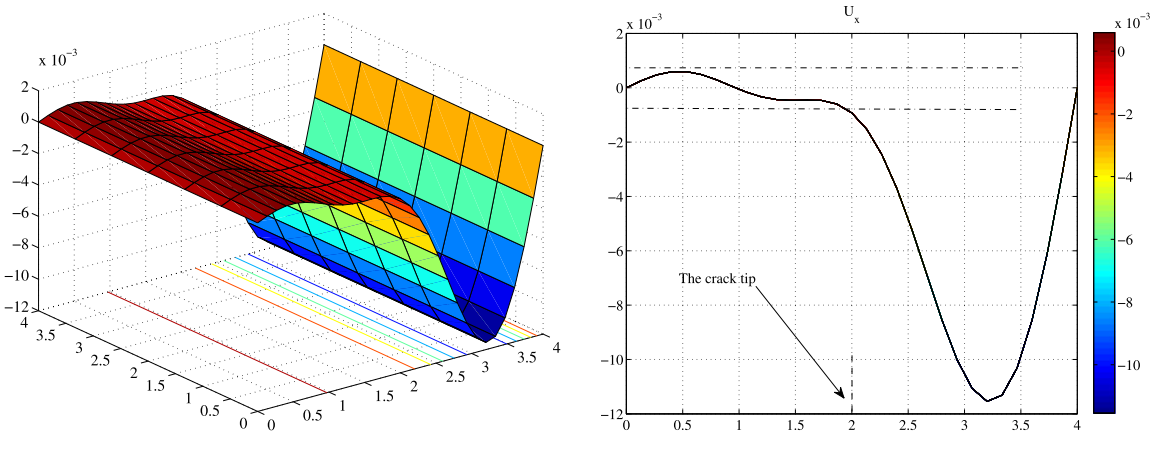

(a) Three dimensional view (b) Cross sectional view in the yx-plane.

Fig. 5. Displacement jump $[\![\tilde{u}_x]\!]$ across the crack of the data completion solution obtained with free noisy data. The dashed lines show how the truncation was done.

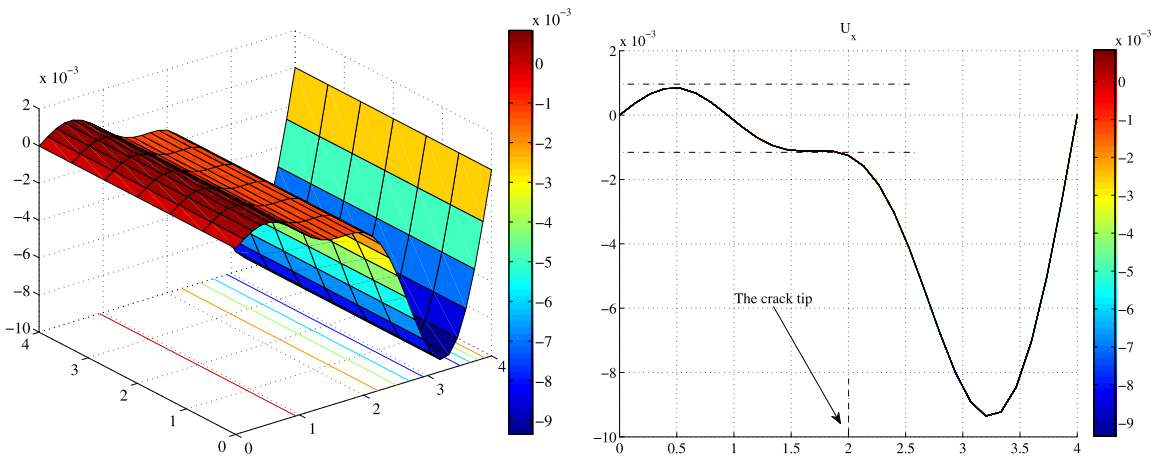

(a) Three dimensional view (b) Cross sectional view in the yx-plane.

Fig. 6. Displacement jump $[\![\tilde{u}_x]\!]$ across the crack of the data completion solution obtained with noisy data (5%). The dashed lines show how the truncation was done.

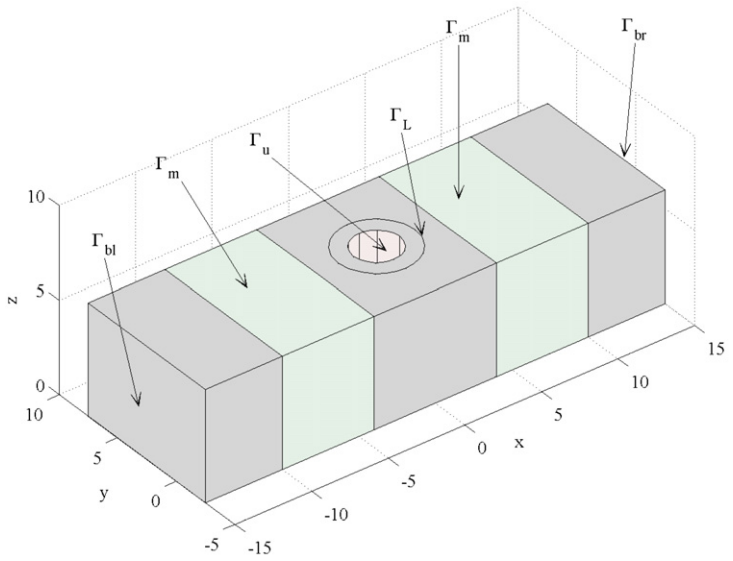

Fig. 7. Domain where the data completion was performed.

area. For this example we follow the following procedure: for each $M \times N$ value the displacement gap (12) is analysed, then the oscillations are truncated so that (12) represents a simply connected area, this is shown in Figs. 8b, 9b and 10b. The procedure is stopped when the oscillations of height frequencies become too important and do not allow us to identify a simply connected area.

The reader can observe that in this case the identified crack front is in good agreement with the reference one. However, in this case, adding 5% noise to the Cauchy data besides the numerical noise due to the data completion process, do not allow the front crack identification.

Fig. 10b depicts the identified domain with a noise level of only 2% on the Dirichlet Cauchy data on Γ_m. It is therefore clear that regularisation procedures are needed in order to improve the results. Note that the noise on Cauchy data induces a stronger noise on the data used in the reciprocity gap step, even on low order modes: in Fig. 10b the overall shape is well recovered whereas the crack area is underestimated, meaning that the error is distributed almost equally on all modes used in the reconstruction of the jump.

6. Conclusions

In this Note, only tangential displacement on the part Γ_m is used because this situation is the more generally encountered when the measurements involve only one DIC. With stereoscopic devices involving two cameras, the full displacement field is available, and the same approach can be used with obvious modifications, this situation is more favourable for the first step of the method (data completion problem) because of the associated increase of data quality and amount.

No regularisation has been used here because of the small number of modes used in the reconstruction of the displacement jump on the crack plane. It appears nevertheless that the ill-posedness of the Cauchy problem [16] affects also the first reconstruction modes of the displacement jumps even if it could have been thought that the computation of RG in the second step of the proposed method involves integrals of the product of the data on Γ_u with values of the trace and traction vector of smooth fields v_{mn} with small values of m and n, and then the products of noise induced high period oscillations in the data with almost non-oscillating field would be almost zero.

Regularisation can be introduced by smoothing up the given or produced fields at the three following steps: first on the measured data on Γ_m, secondly on the trace and traction vector on Γ_u once the Cauchy data is solved, finally on the reconstructed jump $[\![\tilde{u}_x]\!]$ before using the truncating procedure leading to the crack domain identification. In each situation, we will use the following regularised L^2 projection, reading for example for the identified $[\![\tilde{u}_x]\!]$ function:

$$[\![\tilde{u}_x]\!]^r_{MN} = \underset{w\in H^1(\Gamma_u)}{\arg\min} \int_\rho \left([\![\tilde{u}_x]\!]_{MN} - w\right)^2 \mathrm{d}\rho + \varepsilon\sqrt{RH} \int_\rho \sqrt{\nabla w^2 + \alpha^2}\,\mathrm{d}\rho \tag{15}$$

Contrary to the Tikhonov–Phillips regularisation method, this (approximate) total variation semi-norm regularisation method [17] is well suited to damp out the oscillations induced by the limited number of terms in the series while respecting the zones with strong gradients that are crucial for the identification of details in the crack front geometry.

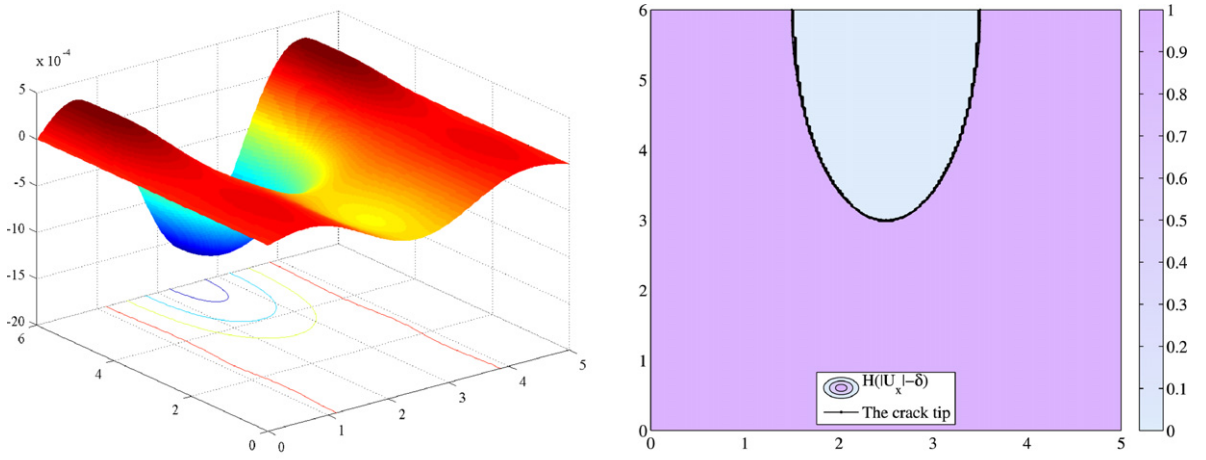

(a) Three dimensional view. (b) Cross sectional view in the yz-plane.

Fig. 8. Displacement jump $[\![\tilde{u}_x]\!]$ across the elliptic crack of the reference solution. The parameter δ is chosen such that γ is simply connected.

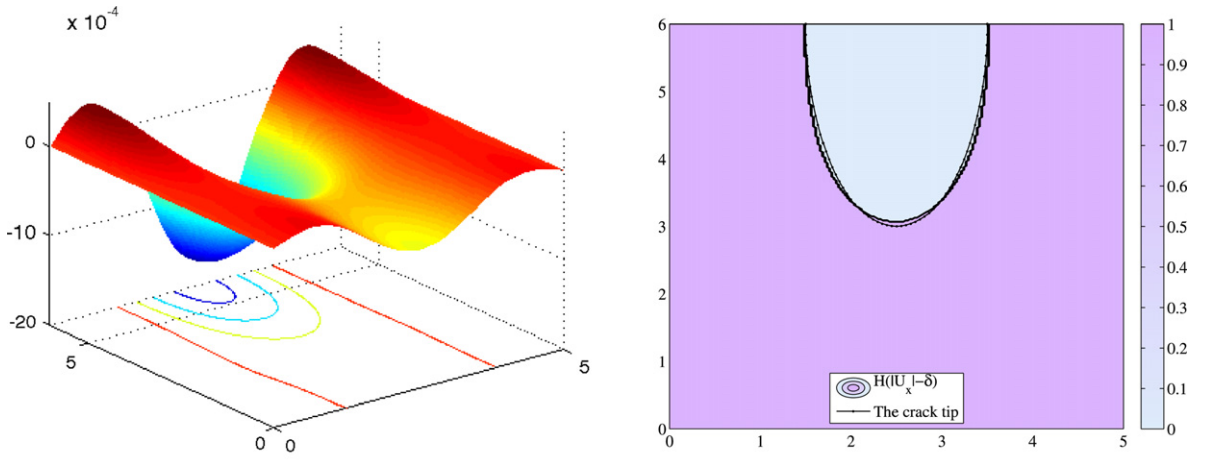

(a) Three dimensional view. (b) Cross sectional view in the yz-plane.

Fig. 9. Displacement jump $[\![\tilde{u}_x]\!]$ across the elliptic crack of the data completion solution obtained with free noisy data. The parameter δ is chosen such that γ is simply connected.

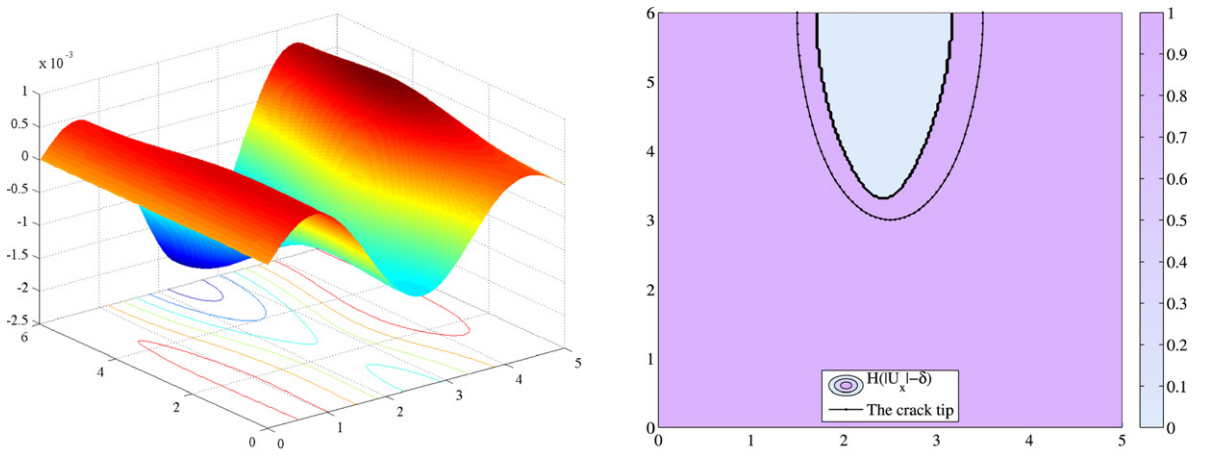

(a) Three dimensional view. (b) Cross sectional view in the yz-plane.

Fig. 10. Displacement jump $[\![\tilde{u}_x]\!]$ across the elliptic crack of the data completion solution obtained with noisy data (2%). The parameter δ is chosen such that γ is simply connected.

References

[1] M.A. Sutton, M. Cheng, W.H. Peters, Y.S. Chao, S.R. McNeill, Application of an optimized digital correlation method to planar deformation analysis, Image Vis. Comput. 4 (1986) 143–150.
[2] B. Wagne, S. Roux, F. Hild, Spectral approach to displacement evaluation from image analysis, Eur. Phys. J., Appl. Phys. 17 (2002) 247–252.
[3] S. Andrieux, T.N. Baranger, Three-dimensional recovery of stress intensity factors and energy release rates from surface full-field measurements, submitted for publication.
[4] J. Réthoré, S. Roux, F. Hild, Noise-robust stress intensity factor determination from kinematic field measurements, Eng. Fract. Mech. 75 (2008) 3763–3781.
[5] S. Yoneyama, T. Ogawa, Y. Kobayashi, Evaluating mixed-mode stress intensity factors from full-field displacement fields obtained by optical methods, Eng. Fract. Mech. 74 (9) (2006) 1399–1412.
[6] M.L. Kadri, J. Ben Abdallah, T.N. Baranger, Identification of internal cracks in a three-dimensional solid body via Steklov–Poincaré approaches, C. R. Mecanique 339 (10) (2011) 674–681.
[7] T.N. Baranger, S. Andrieux, Constitutive law gap functionals for solving the Cauchy problem for linear elliptic PDE, Appl. Math. Comput. 218 (5) (2011) 1970–1989.
[8] S. Andrieux, T.N. Baranger, An energy error-based method for the resolution of the Cauchy problem in 3D linear elasticity, Comput. Methods Appl. Mech. Engrg. 197 (9–12) (2008) 902–920.
[9] T.N. Baranger, S. Andrieux, An optimization approach for the Cauchy problem in linear elasticity, J. Multidiscip. Optim. 35 (2) (2008) 141–152.
[10] S. Andrieux, A. Ben Abda, H.D. Bui, Reciprocity principle and crack identification, Inverse Problems 15 (1) (1999) 59–65.
[11] A. Fursikov, Optimal Control of Distributed Systems—Theory and Applications, Transl. Math. Monogr., vol. 187, American Mathematical Society, Providence, RI, 2000.
[12] R. Rischette, T.N. Baranger, N. Debit, Numerical analysis of an energy-like minimization method to solve the Cauchy problem with noisy data, J. Comput. Appl. Math. 235 (2011) 3257–3269.
[13] H. Brezis, Analyse fonctionnelle : Théorie et applications, Dunod, Paris, 1999.
[14] Comsol Multiphysics, Finite Element Analysis Software, http://www.comsol.com.
[15] MATLAB, The MathWorks Inc., 2012.
[16] F.B. Belgacem, Why is the Cauchy problem severely ill-posed?, Inverse Problems 23 (2007) 823–836.
[17] A. Chambolle, P.L. Lions, Image recovery via total variation minimization and related problems, Numer. Math. 76 (1997) 167–188.